

Breakup temperature of target spectators in $^{197}\text{Au} + ^{197}\text{Au}$ collisions at $E/A = 1000$ MeV

Hongfei Xi^{1,*}, T. Odeh¹, R. Bassini², M. Begemann-Blaich¹, A.S. Botvina^{3,**}, S. Fritz¹, S.J. Gaff⁴, C. Groß¹, G. Immé⁵, I. Iori², U. Kleinevoß¹, G.J. Kunde⁴, W.D. Kunze¹, U. Lynen¹, V. Maddalena⁵, M. Mahi¹, T. Möhlenkamp⁶, A. Moroni², W.F.J. Müller¹, C. Nociforo⁵, B. Ocker⁷, F. Petruzzelli², J. Pochodzalla⁸, G. Raciti⁵, G. Riccobene⁵, F.P. Romano⁵, Th. Rubehn¹, A. Saija⁵, M. Schnittker¹, A. Schüttauf⁷, C. Schwarz¹, W. Seidel⁶, V. Serfling¹, C. Sfienti⁵, W. Trautmann¹, A. Trzcinski⁹, G. Verde⁵, A. Wörner¹, B. Zwieglinski⁹

¹ Gesellschaft für Schwerionenforschung, D-64291 Darmstadt, Germany

² Istituto di Scienze Fisiche, Università degli Studi di Milano and I.N.F.N., I-20133 Milano, Italy

³ Institute for Nuclear Research, Russian Academy of Sciences, 117312 Moscow, Russia

⁴ Department of Physics and Astronomy and National Superconducting Cyclotron Laboratory, Michigan State University, East Lansing, MI 48824, USA

⁵ Dipartimento di Fisica dell'Università and I.N.F.N., I-95129 Catania, Italy

⁶ Forschungszentrum Rossendorf, D-01314 Dresden, Germany

⁷ Institut für Kernphysik, Universität Frankfurt, D-60486 Frankfurt, Germany

⁸ Max-Planck-Institut für Kernphysik, D-69117 Heidelberg, Germany

⁹ Soltan Institute for Nuclear Studies, 00-681 Warsaw, Hoza 69, Poland

Received: 14 March 1997 / Revised version: 29 July 1997

Communicated by V. Metag

Abstract. Breakup temperatures were deduced from double ratios of isotope yields for target spectators produced in the reaction $^{197}\text{Au} + ^{197}\text{Au}$ at 1000 MeV per nucleon. Pairs of $^{3,4}\text{He}$ and $^{6,7}\text{Li}$ isotopes and pairs of $^{3,4}\text{He}$ and H isotopes (p, d and d, t) yield consistent temperatures after feeding corrections, based on the quantum statistical model, are applied. The temperatures rise with decreasing impact parameter from 4 MeV for peripheral to about 10 MeV for the most central collisions.

The good agreement with the breakup temperatures measured previously for projectile spectators at an incident energy of 600 MeV per nucleon confirms the universality established for the spectator decay at relativistic bombarding energies. The measured temperatures also agree with the breakup temperatures predicted by the statistical multifragmentation model. For these calculations a relation between the initial excitation energy and mass was derived which gives good simultaneous agreement for the fragment charge correlations.

The energy spectra of light charged particles, measured at $\theta_{lab} = 150^\circ$, exhibit Maxwellian shapes with inverse slope parameters much higher than the breakup temperatures. The statistical multifragmentation model, because Coulomb repulsion and sequential decay processes are included, yields light-particle spectra with inverse slope parameters higher than the breakup temperatures but considerably below the measured values. The systematic behavior of the differences suggests that they are caused by light-charged-particle emission prior to the final breakup stage.

PACS: 25.70.Mn; 25.70.Pq; 25.75.-q

1 Introduction

Heavy ion reactions at relativistic energies offer a wide range of possibilities to study the multi-fragment decay of highly excited nuclei [1–8]. In collisions of heavy nuclei at incident energies exceeding values of about 100 MeV per nucleon [2], highly excited and equilibrated spectator systems are formed which decay by multifragmentation [9] in good agreement with statistical predictions [10, 11]. The analysis of the kinetic energies of the decay products has not revealed significant flow effects [3, 9, 12]. Therefore, the spectator nuclei which are produced over wide ranges of excitation energy and mass in these reactions, are well suited for the investigation of highly excited nuclear systems in thermodynamical equilibrium.

From the simultaneous measurement of the temperature and the excitation energy for excited projectile spectators in $^{197}\text{Au} + ^{197}\text{Au}$ collisions at 600 MeV per nucleon, a caloric curve of nuclei has recently been obtained [13]. For the temperature determination the method suggested by Albergo et al. has been used which is based on the assumption of chemical equilibrium and requires the measurement of double ratios of isotopic yields [14]. The obtained temperatures, plotted against the measured excitation energy, resulted in a caloric curve with the characteristic behavior reminiscent of first-order phase transitions in macroscopic systems. The 'liquid' and the 'vapor' regimes where the temperature rises with increasing excitation energy are separated by a region of nearly constant temperature $T \approx 5$ MeV over which the multiplicity of the fragmentation products increases. These results and, in particular, the apparent rise of the breakup temperature at excitation energies exceeding 10 MeV per nucleon have initiated a widespread discussion which addresses both methodical aspects and questions of interpretation [15–22].

The qualitative shape of the caloric curve of nuclei has been predicted long ago on the basis of the statistical multifragmentation model [23]. The same model, more recently, has been shown to rather accurately describe the charge cor-

* Present address: National Superconducting Cyclotron Laboratory, Michigan State University, East Lansing, MI 48824, USA

** Present address: Bereich Theoretische Physik, Hahn-Meitner-Institut, D-14109 Berlin, Germany

relations measured for the reaction ^{197}Au on Cu at $E/A = 600$ MeV, including their dispersions around the mean behavior [11]. Naturally, the question arises whether a comparably quantitative level of accuracy can be reached for the reproduction of the measured caloric curve. A statistical description of the spectator decay will only be consistent if the model parameters, including the temperature, are in the range given by the experiment. The breakup temperature should also exhibit the invariance with respect to the entrance channel that has been found for the fragmentation patterns. Their universal dependence on Z_{bound} (Z_{bound} scaling) is a prominent and well established feature of the spectator decay where Z_{bound} , defined as the sum of the atomic numbers Z_i of all projectile fragments with $Z_i \geq 2$, is a quantity closely correlated with the excitation energy imparted to the primary spectator system [9].

In this work, we present results of a new measurement of the breakup temperature in the $^{197}\text{Au} + ^{197}\text{Au}$ reaction, and we address these open questions associated with the statistical interpretation of multi-fragment decays of excited spectators. High-resolution telescopes were used to measure isotopically resolved yields of light charged particles and intermediate-mass fragments emitted by target spectators produced at a bombarding energy of 1000 MeV per nucleon. Methodically, we relied upon the observed isotropy of the spectator decay [9] and replaced the measurement of solid-angle-integrated yields by that of differential yields at selected angles. Temperatures were deduced from double yield ratios of H, He, and Li isotopes whereby feeding corrections, obtained from the quantum statistical model [24, 25], were applied.

The deduced breakup temperatures are compared to those measured previously with the ALADIN spectrometer for the $^{197}\text{Au} + ^{197}\text{Au}$ system at 600 MeV per nucleon [13, 26] and to predictions of a recent version of the statistical multifragmentation model [27]. The input parameters for these calculations were derived from the requirement of a good simultaneous reproduction of the fragment charge correlations. While these comparisons turn out to be rather favourable, it is evident from the measured energy spectra that emission prior to the multi-fragment breakup contributes significantly to the observed light-particle yields.

2 Experimental method

The experiment was performed at the ALADIN spectrometer of the GSI facility [9, 28]. Beams of ^{197}Au of 1000 MeV per nucleon incident energy were provided by the heavy-ion synchrotron SIS and directed onto targets of 25-mg/cm² areal thickness. The present data were taken as part of a larger experiment which incorporated three multi-detector hodoscopes for correlated particle detection, built at INFN-Catania, GSI, and Michigan State University and consisting of a total of 216 Si-CsI(Tl) telescopes [29, 30].

A set of seven telescopes, each consisting of three Si detectors with thickness 50, 300, and 1000 μm and of a 4-cm long CsI(Tl) scintillator with photodiode readout, were used to measure the isotopic yields of light charged particles and fragments. Four telescopes were placed in the forward hemisphere while three telescopes were placed at $\theta_{lab} = 110^\circ$, 130° , and 150° for detecting the products of the target-spectator decay.

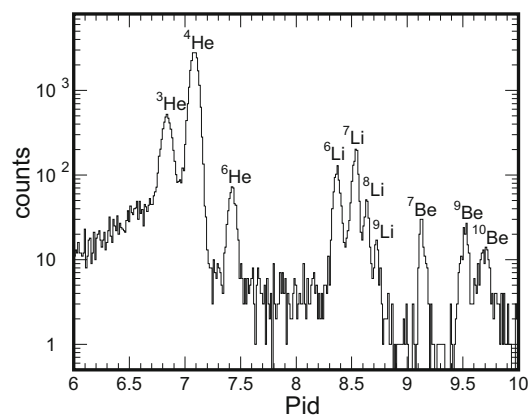


Fig. 1. Spectrum of the particle-identification variable Pid in the range $2 \leq Z \leq 4$ for the telescope positioned at $\theta_{lab} = 150^\circ$. The identified isotopes are indicated

Each telescope subtended a solid angle of 7.0 msr. Permanent magnets were placed next to the entrance collimator of each telescope in order to deflect δ electrons emerging from the target.

For a global characterization of the reaction and impact parameter selection, the quantity Z_{bound} of the coincident projectile decay was measured with the time-of-flight (TOF) wall of the ALADIN spectrometer. Because of the symmetry of the collision system, the mean values of Z_{bound} , for a given event class, should be the same for the target and the projectile spectators. Only very small differences may arise from the finite dispersion of the relation between Z_{bound} and the impact parameter [31].

The energy calibration of the silicon detectors was obtained from the calculated punch-through energies for several isotopes. Radioactive sources of α particles were also used. For the CsI(Tl) detectors, energy calibration was achieved by using the calculated punch-through energies of protons, deuterons, and tritons, the calculated energies of particles whose energy loss was measured with the preceding Si detector, and theoretical light-output curves [32, 33].

The quality of the obtained particle identification is illustrated in Fig. 1 for the case of the telescope placed at $\theta_{lab} = 150^\circ$. Isotopes in the range from hydrogen to carbon were satisfactorily resolved. Isotopic yields were determined by Gaussian fitting with background subtraction. The yields of particles not stopped in the CsI(Tl) detectors was very low at these backward angles and did not affect the deduced isotope ratios. The contamination of lithium yields by two- ^4He events (decay of ^8Be) was estimated to be 2% and ignored. However, because of the presumably different shapes of ^3He and ^4He spectra at low energies (cf. [22, 34, 35]), a correction was required in order to compensate for the effect of the detection threshold $E \approx 12$ MeV for helium, resulting from triggering with the 300- μm detector. The extrapolation to zero threshold energy was based on Maxwellian spectra shapes fitted to the measured parts of the spectra (Fig. 2, full lines). The systematic uncertainty associated with this procedure was assessed by comparing to other methods of extrapolation. An upper limit of the $^3\text{He}/^4\text{He}$ yield ratio was obtained from a data set composed of events triggered by other detectors and extending down to the identification threshold for helium of

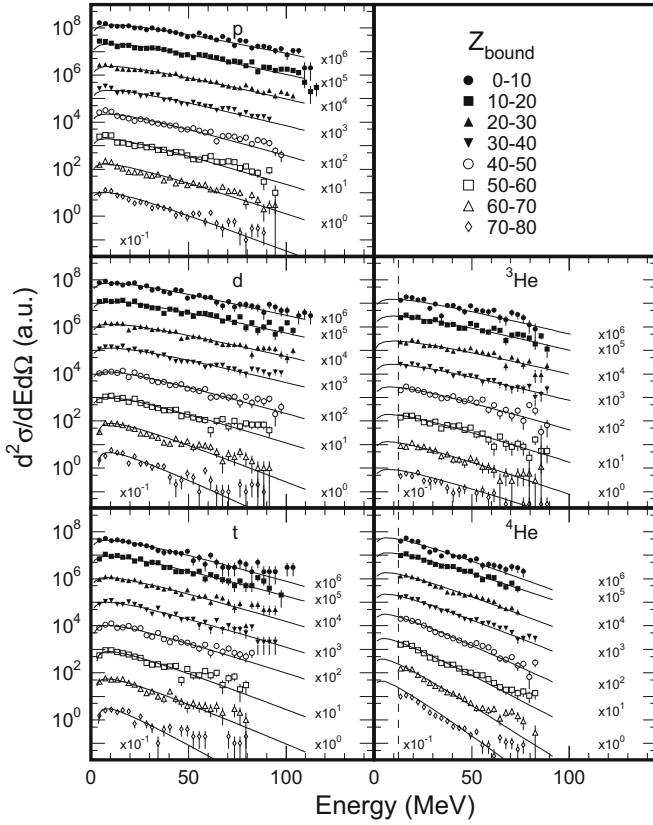


Fig. 2. Energy spectra for hydrogen and helium isotopes, measured at $\theta_{lab} = 150^\circ$, for 10-unit-wide bins in Z_{bound} . All spectra are normalized with respect to each other, note however the scaling factors of powers of 10. The *solid lines* are the results of thermal-source fits, the *dashed line* indicates the trigger threshold of the telescopes for helium ions

$E \approx 8$ MeV. A lower limit was obtained by choosing different energy thresholds $E \geq 12$ MeV in the off-line analysis and by linearly extrapolating the resulting isotope ratios to zero threshold height. The linear extrapolation overestimates the threshold effect because the particle intensities should decrease at very small energies. For these extrapolations of the helium yield ratio, the fitted and background corrected yields as obtained from the identification spectra were used.

For the hydrogen and lithium isotopes, extrapolations to zero threshold were not considered necessary and the measured yield ratios above threshold were used. The experimental thresholds are sufficiently low for the hydrogens and, in the lithium case, a significant mass dependence of the energy spectra was neither expected nor found. This is illustrated in Fig. 3. The curve derived from fitting the spectrum of ${}^7\text{Li}$ ions describes very well also that of ${}^6\text{Li}$ (left panel). The ${}^6\text{Li}/{}^7\text{Li}$ yield ratio does not change significantly as a function of the applied threshold energy (right panel).

3 Experimental results and discussion

3.1 Experimental temperatures

Emission temperatures T were deduced from the double ratios R of yields Y_i measured for pairs of neighboring H, He, or Li

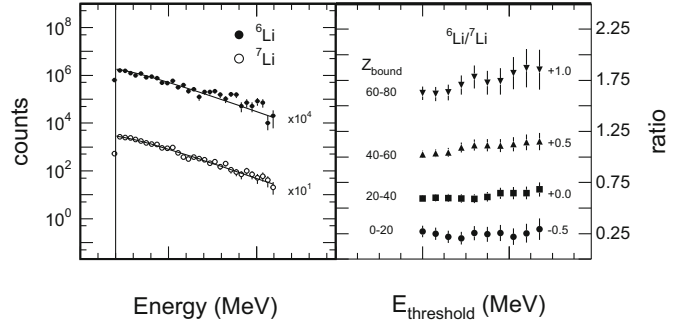


Fig. 3. Energy spectra of ${}^{6,7}\text{Li}$ ions, measured at $\theta_{lab} = 150^\circ$ (left panel), and their yield ratios as a function of the applied energy threshold (right panel). The energy spectra are integrated over the full range of Z_{bound} , the ratios are given for four bins of Z_{bound} as indicated (note the linear offsets). The Maxwellian fit of the ${}^7\text{Li}$ spectrum is shown overlaid over the ${}^6\text{Li}$ spectrum, after an adjustment of the overall yield factor (*full lines*). The trigger threshold of the 300- μm detector is indicated by the *dashed line*

isotopes. Under the assumption of chemical equilibrium, they may be expressed as

$$R = \frac{Y_1/Y_2}{Y_3/Y_4} = a \cdot \exp(((B_1 - B_2) - (B_3 - B_4))/T). \quad (1)$$

Here B_i denotes the binding energy of particle species i and the constant a contains the ground-state spins and mass numbers. For the ratios to be sufficiently sensitive to temperature the double difference of the binding energies

$$b = (B_1 - B_2) - (B_3 - B_4) \quad (2)$$

should be larger than the typical temperature to be measured [20]. In this work we chose ${}^3\text{He}/{}^4\text{He}$ as one of the two ratios (the difference in binding energy is 20.6 MeV) which was combined with either the lithium yield ratio ${}^6\text{Li}/{}^7\text{Li}$ or with the hydrogen yield ratios p/d or d/t . The set of ${}^3\text{He}$, ${}^4\text{He}$, ${}^6\text{Li}$, and ${}^7\text{Li}$ isotopes is the one used previously for the determination of breakup temperatures of projectile spectators in ${}^{197}\text{Au} + {}^{197}\text{Au}$ at 600 MeV per nucleon [13]. Combinations involving p , d , or t , together with ${}^3\text{He}$ and ${}^4\text{He}$, have the advantage of larger production cross sections, particularly in the 'vapor' regime where the heavier fragments are becoming rare.

The four yield ratios used in this work are shown in Fig. 4 as a function of Z_{bound} . For ${}^3\text{He}/{}^4\text{He}$ the systematic errors corresponding to the two limits of extrapolation, described in the previous section, are indicated by the brackets. The particular sensitivity of this ratio is evident; with decreasing Z_{bound} , i.e. increasing centrality, it increases by about one order of magnitude while the other three ratios exhibit a weak and qualitatively similar dependence on Z_{bound} .

Solving (1) with respect to T yields the following three expressions:

$$T_{\text{HeLi},0} = 13.3 / \ln(2.2 \frac{Y_{6\text{Li}}/Y_{7\text{Li}}}{Y_{3\text{He}}/Y_{4\text{He}}}) \quad (3)$$

and

$$T_{\text{HePd},0} = 18.4 / \ln(5.6 \frac{Y_{1\text{H}}/Y_{2\text{H}}}{Y_{3\text{He}}/Y_{4\text{He}}}) \quad (4)$$

and

$$T_{\text{Hedt},0} = 14.3 / \ln(1.6 \frac{Y_{2\text{H}}/Y_{3\text{H}}}{Y_{3\text{He}}/Y_{4\text{He}}}) \quad (5)$$

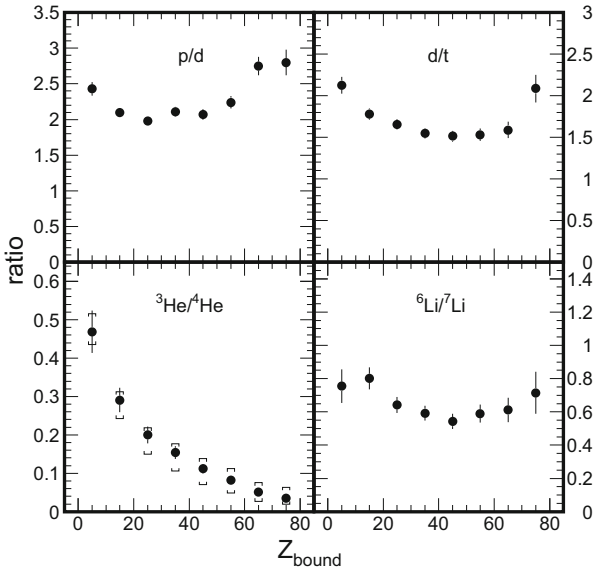


Fig. 4. Four yield ratios of neighbouring H, He, and Li isotopes, measured at $\theta_{lab} = 150^\circ$ and used to deduce breakup temperatures, as a function of Z_{bound} . The error bars represent statistical and the brackets systematic errors (see text)

where the temperatures are given in units of MeV. The subscript 0 is meant to indicate that these apparent temperatures, derived from the measured ground-state populations, may be affected by feeding of these populations from sequentially decaying excited states. The consequences of side feeding are presently a subject of considerable discussion and are quantitatively investigated by several groups with different models [36–39]. Here, the required corrections were calculated with the quantum statistical model which starts from chemical equilibrium at a given temperature, density, and neutron-to-proton (N/Z) ratio and which includes sequential decay [24, 25]. In Fig. 5, the three apparent temperatures defined in (3-5) are shown as a function of the equilibrium temperature T_{input} for the parameters $N/Z = 1.49$ (value of ^{197}Au) and density $\rho = 0.3 \cdot \rho_0$ (where ρ_0 is the saturation density of nuclei). The relations between $T_{\text{HeLi},0}$ or $T_{\text{Hedt},0}$ and T_{input} are almost linear and the corrections required in these two cases are practically identical, except at the highest temperatures. The linear approximation, indicated by the dotted line, corresponds to the constant correction factor $T = 1.2 \cdot T_0$ adopted for T_{HeLi} in [13]. The figure also demonstrates that $T_{\text{Hepd},0}$ is, apparently, more strongly affected by feeding effects at the higher temperatures. In this case, the double ratio includes the yield of protons which are likely to be produced in the decay of excited light fragments. Within the range of densities $0.1 \leq \rho/\rho_0 \leq 0.5$, the corrections required according to the quantum statistical model vary within about $\pm 15\%$ [26]. They virtually do not change with the N/Z ratio of the primary source. In the analysis, the corrections calculated for $\rho/\rho_0 = 0.3$, as derived from the results shown in Fig. 5, were applied.

The side-feeding predictions obtained by other groups [36–39] suggest that the corrections are model dependent. In the region of low excitation energies, the correction factors required for T_{HeLi} range from 1.0 to 1.3, within the uncertainties of the model assumptions. However, at high excitation energies where the consequences of side feeding from higher

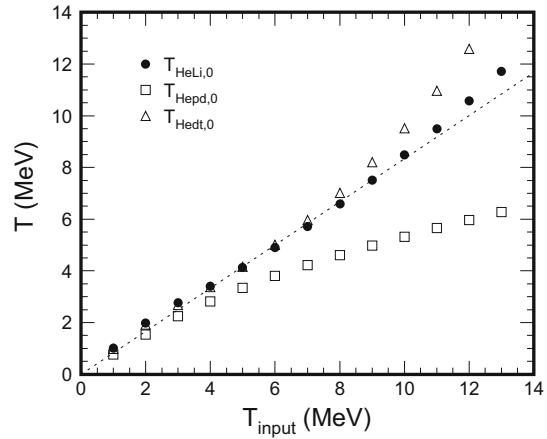


Fig. 5. Apparent temperatures $T_{\text{HeLi},0}$, $T_{\text{Hepd},0}$, and $T_{\text{Hedt},0}$, according to the quantum statistical model, as a function of the input temperature T_{input} . A breakup density $\rho/\rho_0 = 0.3$ is assumed. The dotted line represents the linear relation $T_0 = T_{input}/1.2$

lying states may become more important, the results differ considerably and depend on the amount of unbound states in the continuum that are considered [37, 39] and on the assumed breakup density [26, 38, 39]. In the present work, we use the corrections obtained from the quantum statistical model in order to be consistent with previous analyses. We will also refer to the statistical multifragmentation model which predicts a very similar relation between T_{HeLi} and the equilibrium temperature (Sect. 3.2).

In Fig. 6 the obtained temperatures T_{HeLi} , T_{Hepd} , and T_{Hedt} are shown as a function of Z_{bound} . They are based on the yield ratios measured with the telescope at the most backward angle $\theta_{lab} = 150^\circ$. Simulations indicate that, at this angle, contributions from the midrapidity source should be small. Z_{bound} was determined from the fragments of the projectile decay measured for the same event. The temperatures increase continuously with decreasing Z_{bound} from $T = 4$ MeV for peripheral collisions to about 10 MeV for the most central collisions as-

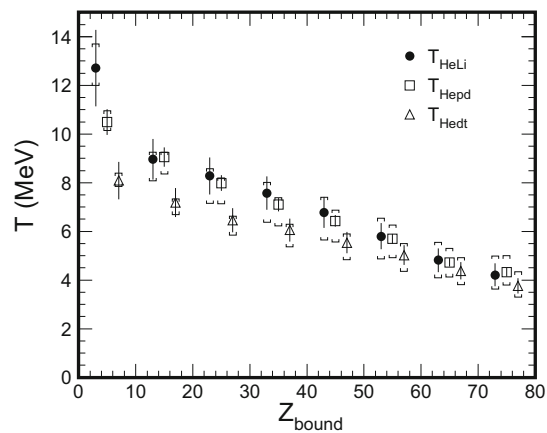


Fig. 6. Temperatures T_{HeLi} , T_{Hepd} , and T_{Hedt} as a function of Z_{bound} , averaged over bins of 10-units width. Corrections have been applied as described in the text. The error bars represent the statistical uncertainty. The systematic uncertainty, caused by the extrapolation of the yields of helium isotopes below the identification threshold, is indicated by the brackets. For clarity, T_{HeLi} and T_{Hedt} are laterally displaced by 2 units of Z_{bound}

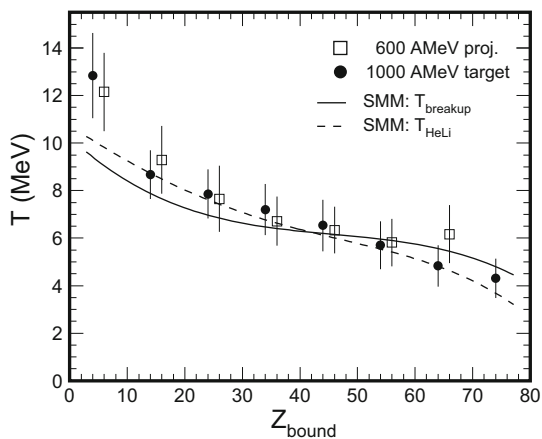


Fig. 7. Temperatures T_{HeLi} of the target spectator from the present experiment at $E/A = 1000$ MeV (dots) and of the projectile spectator at $E/A = 600$ MeV (open squares) as a function of Z_{bound} . The data symbols represent averages over bins of 10-units width and, for clarity, are laterally displaced by 1 unit of Z_{bound} . Statistical and systematic contributions are included in the displayed errors. The lines are smoothed fit curves describing the breakup temperature T_{breakup} (full line) and the isotopic temperature T_{HeLi} (dashed line) calculated with the statistical multifragmentation model. Note that the trigger threshold affected the data of [13, 26] at $Z_{\text{bound}} \geq 65$

sociated with the smallest Z_{bound} values. The range $Z_{\text{bound}} \leq 20$ corresponds to the high excitation energies at which the upbend of the temperature appears in the caloric curve [13]. We note here that the cross section for $Z_{\text{bound}} < 2$ is of the order of 130 mb in this reaction [9] so that the minimum impact parameter for $Z_{\text{bound}} \geq 2$ (partitions with at least one fragment of $Z \geq 2$) is more than 2 fm in a sharp cutoff approximation.

The results obtained with the three different double ratios agree rather well. Only the strong rise of T_{HeLi} at small Z_{bound} is not equally followed by the other two temperatures. T_{HeLi} and T_{HePd} track each other rather closely which is remarkable in view of the different feeding corrections (Fig. 5). Only T_{HeDt} is systematically somewhat lower than the other two temperatures. T_{HeDt} has also been reported to be lower than T_{HeLi} in [21], in agreement with the statistical-model calculations of [39], but has been found to be slightly higher than T_{HeLi} in [7]. It seems difficult to assess the precise nature of these deviations at the present time.

A comparison of the T_{HeLi} temperatures with those derived in previous work for projectile spectators in $^{197}\text{Au} + ^{197}\text{Au}$ collisions at 600 MeV per nucleon is given in Fig. 7. In the case of the projectile decay, the isotopes were identified by tracking of their trajectories with the upgraded TP-MUSIC detector and subsequent momentum and time-of-flight analysis [13, 26]. The displayed data symbols represent the mean values of the range of systematic uncertainties associated with the two different experiments while the errors include both statistical and systematic contributions. The projectile temperatures are the result of a new analysis of the original data and are somewhat higher, between 10% and 20%, than those reported previously. Their larger errors follow from a reassessment of the potential ^4He contamination of the ^6Li yield caused by Z misidentification.

Within the errors, good agreement is observed for the results at 600 and 1000 MeV per nucleon. The expected invariance of the breakup temperature with the bombarding energy

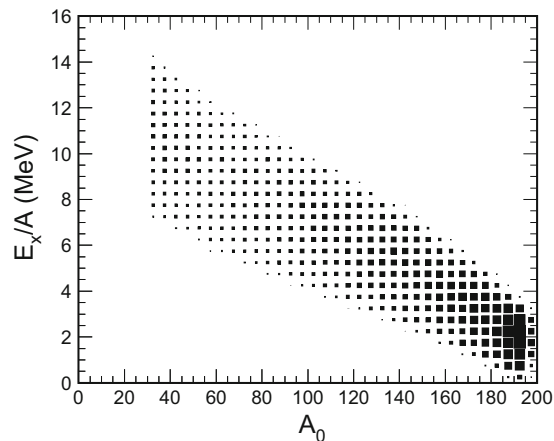


Fig. 8. Excitation energy E_x/A as a function of the mass A_0 for the ensemble of excited spectator nuclei used as input for the calculations with the statistical multifragmentation model. The area of the squares is proportional to the intensity

is thus confirmed. It is consistent with the Z_{bound} scaling of the mean fragment multiplicities and charge correlations and supports the statistical interpretation of the multi-fragment decay of highly excited spectator nuclei [9]. The breakup temperatures deduced by the EOS collaboration for $^{197}\text{Au} + \text{C}$ at 1 GeV per nucleon are also consistent with this conclusion [7]. Within the range $Z_{\text{bound}} \geq 40$ which is mainly populated in this reaction [9], they are in agreement with the present results for $^{197}\text{Au} + ^{197}\text{Au}$, both in absolute magnitude and in their dependence on the impact parameter, and thus confirm the expected invariance with respect to the mass of the collision partner.

3.2 Model calculations

The calculations within the statistical multifragmentation model [27] were performed in order to test its consistency with respect to the statistical parameters and predicted charge partitions. Here one assumes that all observed particles come from the decay of one equilibrated source. The correlation of excitation energy and mass of the ensemble of excited spectator nuclei, required as input for the calculations, was chosen in the form shown in Fig. 8. The neutron-to-proton ratio was taken to be that of ^{197}Au ($N/Z = 1.49$). The distribution of excitation energies at fixed spectator mass A_0 had a Gaussian width, chosen in proportion to the square root of the mean excitation energy, and the distribution of masses A_0 was adjusted in order to reproduce the measured cross section $d\sigma/dZ_{\text{bound}}$.

As a criterion for setting the excitation energy per nucleon, E_x/A , we chose the capability of the model to simultaneously describe the correlations of the mean multiplicity $\langle M_{\text{IMF}} \rangle$ of intermediate-mass fragments (IMF's) and of the mean charge asymmetry $\langle a_{12} \rangle$ with Z_{bound} . The asymmetry a_{12} of the two largest fragments is defined as $a_{12} = (Z_{\text{max}} - Z_2)/(Z_{\text{max}} + Z_2)$, with the mean value to be calculated from all events with $Z_{\text{max}} \geq Z_2 \geq 2$. The comparison, shown in Fig. 9, was based on the data reported in [9]. In the region $Z_{\text{bound}} > 30$, the mean excitation energy of the ensemble of spectator nuclei was found to be well constrained by the mean fragment

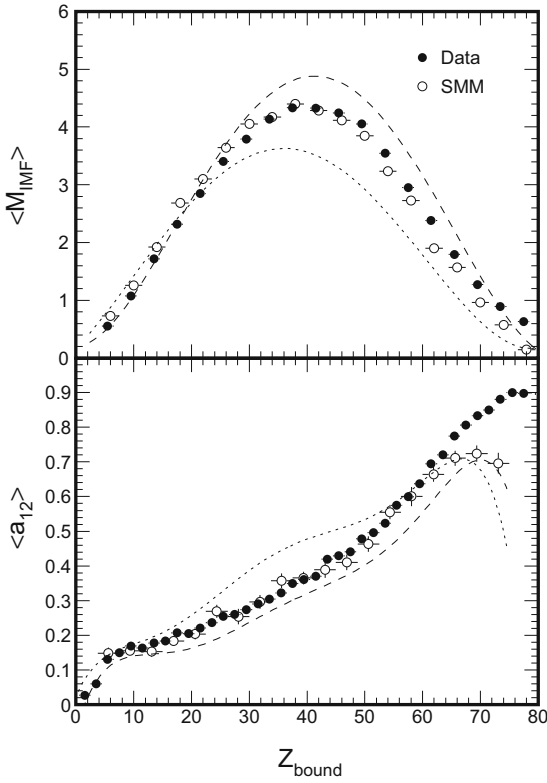


Fig. 9. Mean multiplicity of intermediate-mass fragments $\langle M_{IMF} \rangle$ (top) and mean charge asymmetry $\langle a_{12} \rangle$ (bottom) as a function of Z_{bound} , as obtained from the calculations with the statistical multifragmentation model (open circles) in comparison to the experiment (dots, from [9]). The dashed and dotted lines show the results of the calculations with excitation energies E_x/A 15% above and 15% below the adopted values, respectively. Note that the trigger threshold affected the data of ref. [9] at $Z_{bound} \geq 65$

multiplicity alone. At $Z_{bound} \approx 30$ and below, the charge asymmetry was a necessary second constraint (cf. [40]) while, at the lowest values of Z_{bound} , neither the multiplicity nor the asymmetry provided rigid constraints on the excitation energy. These sensitivities are illustrated in Fig. 9 where the dashed and dotted lines show the model results for E_x/A chosen 15% above and below the adopted values.

The excitation energies that have resulted from this procedure are somewhat larger than those found previously in analyses [40–42] of the earlier ^{197}Au on Cu data at 600 MeV per nucleon [43]. The difference reflects the sensitivity to the fragment multiplicity and is caused by the slightly larger mean multiplicities that were obtained from the more recent experiments with improved acceptance [9]. The excitation energies are still smaller than the experimental values obtained with the calorimetric method of summing up the kinetic energies of the product nuclei and their mass excess with respect to the ground state of the original spectator system [9, 13].

The calculations proceed such that, for a given mass, charge, and excitation energy, first the partition function is calculated and then the temperature $T = \langle T_f \rangle$ is obtained as the average over the ensemble of partitions. In the micro-canonical approximation, the temperature T_f for a particular partition f is found from the energy balance

$$E_f(T_f, V) = E_0 \quad (6)$$

where E_f is the energy of the system at T_f within the volume V , and E_0 is the total available energy [27]. At high excitation energies, when the system disassembles into many fragments, this temperature is very close to the grand canonical temperature.

The solid line in Fig. 7 represents the thermodynamical temperature T obtained in this way from the calculations. With decreasing Z_{bound} , it increases monotonically from about 5 to 9 MeV. Over a wide range of Z_{bound} it remains close to $T = 6$ MeV which reflects the plateau predicted by the statistical multifragmentation model for the range of excitation energies $3 \text{ MeV} \leq E_x/A \leq 10 \text{ MeV}$ [27]. In model calculations performed for a fixed spectator mass, the plateau is associated with a strong and monotonic rise of the fragment multiplicities. Experimentally, due to the decrease of the spectator mass with increasing excitation energy, the production of intermediate-mass fragments passes through a maximum in the corresponding range of Z_{bound} of about 20 to 60 (cf. Figs. 8, 9).

The dashed line gives the temperature T_{HeLi} obtained from the calculated isotope yields. Because of sequential feeding, it differs from the thermodynamical temperature, the uncorrected temperature $T_{\text{HeLi},0}$ being somewhat lower. Here, in order to permit the direct comparison with the experimental data in one figure, we display T_{HeLi} which has been corrected in the same way with the factor 1.2 suggested by the quantum statistical model. The model T_{HeLi} exhibits a more continuous rise with decreasing Z_{bound} than the thermodynamical temperature and is in very good agreement with the measured values. We thus find that, with the parameters needed to reproduce the observed charge partitions, this temperature-sensitive observable is well reproduced. In the bin $Z_{bound} \leq 10$ the model values fall below the data. Here, the experimental uncertainty is rather large but the constraint on the excitation energy provided by the charge partitions is also rather weak (see above). The discrepancy may therefore indicate that the excitation energies for breakups corresponding to this bin of Z_{bound} may be higher than assumed in the calculations.

The correction applied to the calculated T_{HeLi} (dashed line) results in a good overall agreement with the equilibrium temperature of the model calculations (full line). This means that the side-feeding corrections suggested by the statistical multifragmentation model and by the quantum statistical model are qualitatively very similar. The difference between them is given by the deviations of the two curves. They range from about +20% at large Z_{bound} to -10% at small Z_{bound} and thus stay within the range of model uncertainties quoted above. They may reflect finite size effects, ignored in the quantum statistical model, and their variation as the spectator mass changes as a function of Z_{bound} [13]. They can, equally well, be interpreted as indicating a variation of the breakup density with Z_{bound} . In the region of small Z_{bound} , i.e. at temperatures of about 8 to 10 MeV the correction factors of the quantum statistical model are lowered by 10% if the density is chosen to be $\rho/\rho_0 = 0.15$ instead of 0.3. A decrease of the breakup density of that order, as Z_{bound} decreases from near 40 to below 20, does not seem unreasonable. One may therefore expect that an analysis based on measured breakup densities (cf. [38]) will bring T_{HeLi} into even better agreement with the equilibrium temperatures obtained with the statistical multifragmentation model.

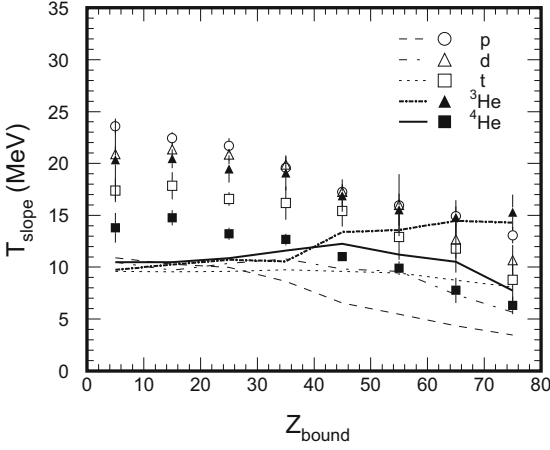


Fig. 10. Inverse slope parameters T_{slope} for hydrogen and helium isotopes, obtained from fits to the measured (data symbols, $\theta_{lab} = 150^\circ$) and calculated (lines) energy spectra, as a function of Z_{bound}

3.3 Energy spectra

The kinetic energy spectra were studied for light charged particles up to ${}^4\text{He}$. For the five species proton, deuteron, triton, ${}^3\text{He}$, and ${}^4\text{He}$, the spectra measured at $\theta_{lab} = 150^\circ$ and sorted according to Z_{bound} are shown in Fig. 2. Fit results, based on a single target spectator source, are given by the full lines. They were obtained by assuming that all the particle spectra have Maxwellian shapes

$$dN/dE \sim \sqrt{E - V_C} \cdot e^{-(E - V_C)/T} \quad (7)$$

where V_C is the effective Coulomb barrier and T is the temperature. The smearing of the spectra in the low-energy region due to the finite target thickness and a possible motion of the target source (at the most a few percent of the speed of light, see [9]) were ignored since their effect on the temperature parameters is too small as to be important for the following discussion.

The inverse slope parameters T_{slope} obtained from the fits are shown in Fig. 10 as a function of Z_{bound} . These kinetic temperatures also increase with decreasing Z_{bound} , consistent with increasing energy deposition, but their absolute values are much higher than the breakup temperatures deduced from the isotope yield ratios or from the model description. There is also a tendency to saturate in the $Z_{bound} \leq 20$ region. Evidently, the inverse slope parameters are not closely related to the breakup temperatures.

The slope parameters of the kinetic-energy spectra calculated with the statistical multifragmentation model are given by the lines shown in Fig. 10. For the range of $Z_{bound} \leq 30$ they are in the vicinity of 10 MeV and nearly the same for the five particle species. This value is considerably higher than the internal temperatures at breakup (cf. Fig. 7, full line) which reflects the additional fluctuations due to Coulomb repulsion and secondary decays after breakup, to the extent that these effects are incorporated in the model. Apparently, they account for only part of the difference to the experimental slopes. Towards larger values of Z_{bound} , the model results start to spread out over the range 5 to 15 MeV, with the protons exhibiting the lowest and ${}^3\text{He}$ the highest inverse slope parameters.

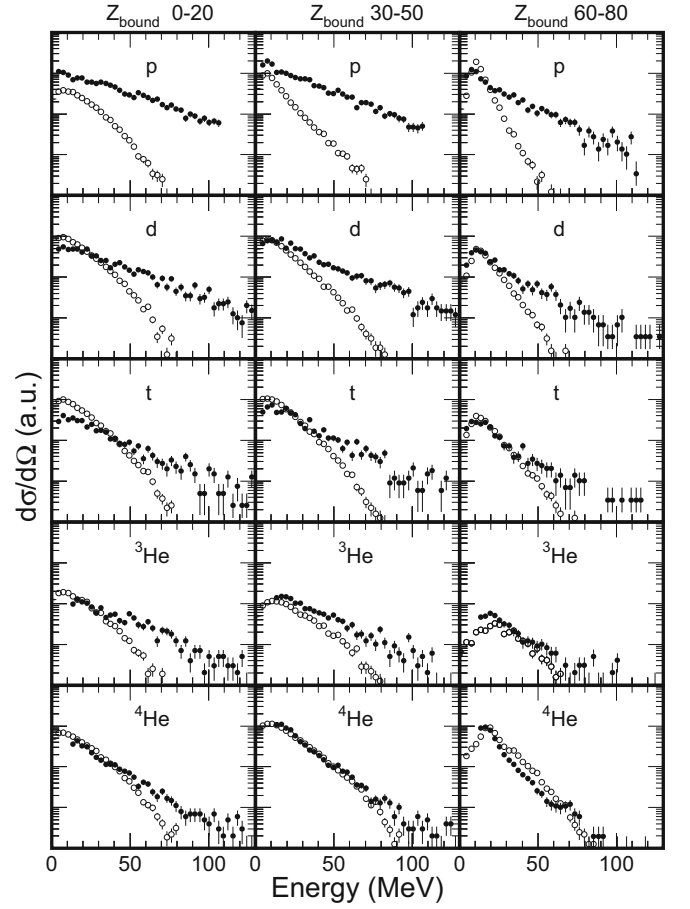


Fig. 11. Energy spectra, measured at $\theta_{lab} = 150^\circ$, of light charged particles p, d, t, ${}^3\text{He}$, and ${}^4\text{He}$ for three intervals of Z_{bound} as indicated. The dots represent the measured spectra, the open circles are the results of the calculations with the statistical multifragmentation model. The spectra are normalized as stated in the text

In Fig. 11, the measured kinetic energy spectra, integrated over finite ranges of Z_{bound} , are shown in comparison to the model results. The two sets of experimental and model spectra are each normalized separately, and one overall normalization factor is used to relate the two sets. It was adapted to the yields of $Z = 2$ fragments because their calculated multiplicities, as a function of Z_{bound} , are found to satisfactorily reproduce the experimental multiplicities reported in [9].

The main trend apparent from the comparison is a systematically increasing deviation of the experimental from the model spectra with decreasing Z_{bound} , i.e. increasing centrality, and with decreasing particle mass. It not only affects the slope parameters describing the shape of the spectra but also the integrated intensities. The yields of hydrogen isotopes, and in particular of the protons, are grossly underestimated by the statistical multifragmentation model. In the case of ${}^4\text{He}$, on the other hand, the equilibrium description accounts rather well for the multiplicities and kinetic energies. A major contribution to the observed ${}^4\text{He}$ yields is expected to come from evaporation by large fragments and excited residue-like nuclei which, apparently, is modelled well.

Conceivable mechanisms that cannot explain the observed deviations include collective flow and Coulomb effects which both should act in proportion to the mass or charge of the emit-

ted particle, contrary to what is observed. On the other hand, the commonly adopted scenario of freeze-out after expansion involves a pre-breakup phase during which the system cools not only by adiabatic expansion but also by the emission of light particles, predominantly nucleons but also light complex particles [41, 44, 45]. The spectra should reflect the higher temperatures at the earlier stages of the reaction, prior to the final breakup into fragments. In addition, there may be contributions from the primary dynamical stage of the reaction, not as much from the mid-rapidity source itself than from secondary scatterings with spectator nucleons. This picture is in line with the fact that higher excitation energies were deduced from the experimental data [9, 13] than were needed as input for the calculations (Fig. 8). Further investigations of the pre-breakup emission will be necessary in order to clarify this problem (see also [7, 46]).

A significant component of pre-breakup emission in the light particle yields has two consequences that deserve particular attention. The pre-breakup yields of protons, deuterons, and tritons are included in the double ratios used to determine the temperatures T_{Hepd} and T_{Hedt} . This violates the requirement of thermal and chemical equilibrium, which is the basic assumption of the method, and thus may shed doubt on the meaning of the consistency exhibited in Fig. 6. On the other hand, the deduced temperatures reflect mainly the sensitivity of the ${}^3\text{He}/{}^4\text{He}$ yield ratio. The p/d ratio varies rather slowly with temperature, as evident from Fig. 4 and also predicted by the quantum statistical model. Therefore, the overall p/d ratio and the deduced temperatures should not be strongly affected by contributions to the hydrogen yields from earlier reaction stages. The second point concerns the excitation energy carried away prior to the equilibrium breakup. Part of this energy may be included in a calorimetric measurement of the spectator excitation. This has to be taken into account in the interpretation of the resulting experimental caloric curve.

4 Conclusion and outlook

Breakup temperatures T_{HeLi} , T_{Hepd} , and T_{Hedt} were measured for target spectators in ${}^{197}\text{Au} + {}^{197}\text{Au}$ collisions at 1000 MeV per nucleon. In these reactions multifragmentation is the dominant decay channel of the produced spectator systems over a wide range of excitation energy and mass. The corrections for sequential feeding of the ground-state yields, based on calculations with the quantum statistical model, resulted in mutually consistent values for the three temperature observables, except in the range of very small Z_{bound} .

With decreasing Z_{bound} , the obtained temperatures increase from $T = 4$ MeV for peripheral collisions to about 10 MeV for the most central collisions. Within the errors, the values for T_{HeLi} are in good agreement with those measured with the ALADIN spectrometer for projectile spectators in the same reaction at 600 MeV per nucleon. This invariance of the breakup temperature with the bombarding energy is consistent with the observed Z_{bound} scaling of the mean fragment multiplicities and charge correlations and supports the statistical interpretation of the multi-fragment decay of highly excited spectator nuclei.

The comparison with the results of calculations within the statistical multifragmentation model shows that a good si-

multaneous agreement for the charge partitions and for the breakup temperatures can be achieved. A necessary requirement for a consistent statistical description of the spectator fragmentation is thus fulfilled. The obtained equilibrium temperature increases less steeply with increasing centrality and stays close to $T = 6$ MeV over a wide range of Z_{bound} , coinciding with the maximum multiplicity of intermediate-mass fragments. In the bin of smallest Z_{bound} , the strong rise of the experimental T_{HeLi} to 12 MeV is not followed by the model prediction but neither is the excitation energy, used as input for the model calculations, well constrained for very small Z_{bound} . The side-feeding corrections obtained with the quantum statistical model and with the statistical multifragmentation model are in qualitative agreement. The remaining differences may largely disappear if a variation of the breakup density with impact parameter is considered in applying the quantum statistical model. T_{HeLi} for small Z_{bound} will then be lowered accordingly.

The T_{slope} parameters characterizing the calculated particle spectra, although higher than the breakup temperatures, are still considerably smaller than the experimental values. The systematic increase of the deviations with decreasing particle mass indicates that they may be caused by light-particle emission prior to the final breakup stage. A more quantitative understanding of the role of the pre-breakup processes will be essential for the interpretation of temperatures obtained from light-particle yields as well as of the excitation energies obtained from calorimetric measurements of the spectator source.

The authors wish to thank the staff at SIS and GSI for the excellent working conditions and J. Lühning and W. Quick for technical support. We are grateful to J. Konopka for providing us with the results of quantum-statistical-model calculations. J.P. and M.B. acknowledge the financial support of the Deutsche Forschungsgemeinschaft under the Contract No. Po 256/2-1 and Be1634/1-1, respectively. This work was supported by the European Community under contract ERBFMGECT950083.

References

1. C.A. Ogilvie, J.C. Adloff, M. Begemann-Blaich, P. Bouissou, J. Hubele, G. Immé, I. Iori, P. Kreutz, G.J. Kunde, S. Leray, V. Lindenstruth, Z. Liu, U. Lynen, R.J. Meijer, U. Milkau, W.F.J. Müller, C. Ngó, J. Pochodzalla, G. Raciti, G. Rudolf, H. Sann, A. Schüttauf, W. Seidel, L. Stuttgé, W. Trautmann, and A. Tucholski, Phys. Rev. Lett. **67** (1991) 1214
2. M.B. Tsang, W.C. Hsi, W.G. Lynch, D.R. Bowman, C.K. Gelbke, M.A. Lisa, G.F. Peaslee, G.J. Kunde, M.L. Begemann-Blaich, T. Hofmann, J. Hubele, J. Kempter, P. Kreutz, W.D. Kunze, V. Lindenstruth, U. Lynen, M. Mang, W.F.J. Müller, M. Neumann, B. Ocker, C.A. Ogilvie, J. Pochodzalla, F. Rosenberger, H. Sann, A. Schüttauf, V. Serfling, J. Stroth, W. Trautmann, A. Tucholski, A. Wörner, E. Zude, B. Zwieglinski, S. Aiello, G. Immé, V. Pappalardo, G. Raciti, R.J. Charity, L.G. Sobotka, I. Iori, A. Moroni, R. Scardaoni, A. Ferrero, W. Seidel, Th. Blaich, L. Stuttgé, A. Cosmo, W.A. Friedman, and G. Peilert, Phys. Rev. Lett. **71** (1993) 1502
3. W. Trautmann, J.C. Adloff, M. Begemann-Blaich, P. Bouissou, J. Hubele, G. Immé, I. Iori, P. Kreutz, G.J. Kunde, S. Leray, V. Lindenstruth, Z. Liu, U. Lynen, R.J. Meijer, U. Milkau, A. Moroni, W.F.J. Müller, C. Ngó, C.A. Ogilvie, J. Pochodzalla, G. Raciti, G. Rudolf, H. Sann, A. Schüttauf, W. Seidel, L. Stuttgé, and A. Tucholski, Acta Phys. Pol. **B25** (1994) 425
4. W. Reisdorf, D. Best, A. Gobbi, N. Herrmann, K.D. Hildenbrand, B. Hong, S.C. Jeong, Y. Leifels, C. Pinkenburg, J.L. Ritman, D. Schüll, U. Sodan, K. Teh, G.S. Wang, J.P. Wessels, T. Wienold, J.P. Alard,

- V. Amouroux, Z. Basrak, N. Bastid, I. Belyaev, L. Berger, J. Biegan-sky, M. Bini, S. Boussange, A. Buta, R. Čaplár, N. Cindro, J.P. Coffin, P. Crochet, R. Dona, P. Dupieux, M. Dželalija, J. Erő, M. Eskéf, P. Fintz, Z. Fodor, L. Fraysse, A. Genoux-Lubain, G. Goebels, G. Guillaume, Y. Grigorian, E. Häfele, S. Hölbling, A. Houari, M. Ib-nouzahir, M. Joriot, F. Jundt, J. Kecskemeti, M. Kirejczyk, P. Koncz, Y. Korchagin, M. Korolija, R. Kotte, C. Kuhn, D. Lambrecht, A. Lebedev, A. Lebedev, I. Legrand, C. Maazouzi, V. Manko, T. Matulewicz, P.R. Maurenzig, H. Merlitz, G. Mgebrishvili, J. Mönsner, S. Mohren, D. Moisa, G. Montarou, I. Montbel, P. Morel, W. Neubert, A. Olmi, G. Pasquali, D. Pelte, M. Petrovici, G. Poggi, P. Pras, F. Rami, V. Rami-lien, C. Roy, A. Sadchikov, Z. Seres, B. Sikora, V. Simion, K. Siwek-Wilczyńska, V. Smolyankin, N. Taccetti, R. Tezkratt, L. Tizniti, M. Trza-ska, M.A. Vasiliev, P. Wagner, K. Wisniewski, D. Wohlfarth, and A. Zhilin, *Nucl. Phys. A* **612** (1997) 493
5. V. Lips, R. Barth, H. Oeschler, S.P. Avdeyev, V.A. Karnaukhov, W.D. Kuznetsov, L.A. Petrov, O.V. Bochkaev, L.V. Chulkov, E.A. Kuzmin, W. Karcz, W. Neubert, and E. Norbeck, *Phys. Rev. Lett.* **72** (1994) 1604
 6. K. Kwiatkowski, K.B. Morley, E. Renshaw Foxford, D.S. Bracken, V.E. Viola, N.R. Yoder, R. Legrain, E.C. Pollacco, C. Volant, W.A. Fried-man, R.G. Korteling, J. Brzychczyk, and H. Breuer, *Phys. Rev. Lett.* **74** (1995) 3756
 7. J.A. Hauger, S. Albergo, F. Bieser, F.P. Brady, Z. Caccia, D.A. Cebra, A.D. Chacon, J.L. Chance, Y. Choi, S. Costa, J.B. Elliott, M.L. Gilkes, A.S. Hirsch, E.L. Hjort, A. Insolia, M. Justice, D. Keane, J.C. Kint-ner, V. Lindenstruth, M.A. Lisa, U. Lynen, H.S. Matis, M. McMahan, C. McParland, W.F.J. Müller, D.L. Olson, M.D. Partlan, N.T. Porile, R. Potenza, G. Rai, J. Rasmussen, H.G. Ritter, J. Romanski, J.L. Romero, G.V. Russo, H. Sann, R. Scharenberg, A. Scott, Y. Shao, B.K. Srivastava, T.J.M. Symons, M. Tincknell, C. Tuvé, S. Wang, P. Warren, H.H. Wier-man, T. Wienold, and K. Wolf, *Phys. Rev. Lett.* **77** (1996) 235
 8. For a recent review see L.G. Moretto and G.J. Wozniak, *Ann. Rev. Nucl. Part. Science* **43** (1993) 379
 9. A. Schüttauf, W.D. Kunze, A. Wörner, M. Begemann-Blaich, Th. Blaich, D.R. Bowman, R.J. Charity, A. Cosmo, A. Ferrero, C.K. Gelbke, C. Groß, W.C. Hsi, J. Hubele, G. Immé, I. Iori, J. Kemper, P. Kreuzt, G.J. Kunde, V. Lindenstruth, M.A. Lisa, W.G. Lynch, U. Lynen, M. Mang, T. Möhlenkamp, A. Moroni, W.F.J. Müller, M. Neumann, B. Ocker, C.A. Ogilvie, G.F. Peaslee, J. Pochodzalla, G. Raciti, F. Rosenberger, Th. Rubehn, H. Sann, C. Schwarz, W. Seidel, V. Serfling, L.G. Sobotka, J. Stroth, L. Stuttgé, S. Tomasevic, W. Trautmann, A. Trzcinski, M.B. Tsang, A. Tucholski, G. Verde, C.W. Williams, E. Zude, and B. Zwieglinski, *Nucl. Phys. A* **607** (1996) 457
 10. J. Hubele, P. Kreuzt, V. Lindenstruth, J.C. Adloff, M. Begemann-Blaich, P. Bouissou, G. Imme, I. Iori, G.J. Kunde, S. Leray, Z. Liu, U. Lynen, R.J. Meijer, U. Milkau, A. Moroni, W.F.J. Müller, C. Ngô, C.A. Ogilvie, J. Pochodzalla, G. Raciti, G. Rudolf, H. Sann, A. Schüttauf, W. Seidel, L. Stuttgé, W. Trautmann, A. Tucholski, R. Heck, A.R. DeAngelis, D.H.E. Gross, H.R. Jaqaman, H.W. Barz, H. Schulz, W.A. Friedman, and R.J. Charity, *Phys. Rev. C* **46** (1992) R1577
 11. A.S. Botvina, I.N. Mishustin, M. Begemann-Blaich, J. Hubele, G. Immé, I. Iori, P. Kreuzt, G.J. Kunde, W.D. Kunze, V. Lindenstruth, U. Lynen, A. Moroni, W.F.J. Müller, C.A. Ogilvie, J. Pochodzalla, G. Raciti, Th. Rubehn, H. Sann, A. Schüttauf, W. Seidel, W. Trautmann, and A. Wörner, *Nucl. Phys. A* **584** (1995) 737
 12. V. Lindenstruth, PhD thesis, Universität Frankfurt, 1993, report GSI-93-18
 13. J. Pochodzalla, T. Möhlenkamp, T. Rubehn, A. Schüttauf, A. Wörner, E. Zude, M. Begemann-Blaich, Th. Blaich, H. Emling, A. Ferrero, C. Groß, G. Immé, I. Iori, G.J. Kunde, W.D. Kunze, V. Lindenstruth, U. Lynen, A. Moroni, W.F.J. Müller, B. Ocker, G. Raciti, H. Sann, C. Schwarz, W. Seidel, V. Serfling, J. Stroth, W. Trautmann, A. Trzcinski, A. Tucholski, G. Verde, and B. Zwieglinski, *Phys. Rev. Lett.* **75** (1995) 1040
 14. S. Albergo, S. Costa, E. Costanzo, and A. Rubbino, *Il Nuovo Cimento* **89A** (1985) 1
 15. J.B. Natowitz, K. Hagel, R. Wada, Z. Majka, P. Gonthier, J. Li, N. Mdei-wayeh, B. Xiao, and Y. Zhao, *Phys. Rev. C* **52** (1995) R2322
 16. L.G. Moretto, R. Ghetti, L. Phair, K. Tso, and G.J. Wozniak, *Phys. Rev. Lett.* **76** (1996) 2822
 17. M.B. Tsang, F. Zhu, W.G. Lynch, A. Aranda, D.R. Bowman, R.T. de Souza, C.K. Gelbke, Y.D. Kim, L. Phair, S. Pratt, C. Williams, H.M. Xu, and W.A. Friedman, *Phys. Rev. C* **53** (1996) R1057
 18. X. Campi, H. Krivine, and E. Plagnol, *Phys. Lett. B* **385** (1996) 1
 19. A. Kolomiets, V.M. Kolomietz, and S. Shlomo, *Phys. Rev. C* **55** (1997) 1376
 20. M.B. Tsang, W.G. Lynch, H. Xi, and W.A. Friedman, *Phys. Rev. Lett.* **78** (1997) 3836
 21. Y.-G. Ma, A. Siwek, J. Péter, F. Gulminelli, R. Dayras, L. Nalpas, B. Tamain, E. Vient, G. Auger, Ch.O. Bacri, J. Benlliure, E. Bisquer, B. Borderie, R. Bougault, R. Brou, J.L. Charvet, A. Chbihi, J. Colin, D. Cussol, E. De Filippo, A. Demeyer, D. Doré, D. Durand, P. Eco-mard, P. Eudes, E. Gerlic, D. Gourio, D. Guinet, R. Laforest, P. Lattes, J.L. Laville, L. Lebreton, J.F. Lecomte, A. Le Fèvre, T. Lefort, R. Legrain, O. Lopez, M. Louvel, J. Lukasik, N. Marie, V. Métivier, A. Quatizerga, M. Parlog, E. Plagnol, A. Rahmani, T. Reposeur, M.F. Rivet, E. Rosato, F. Saint-Laurent, M. Squalli, J.C. Steckmeyer, M. Stern, L. Tassan-Got, C. Volant, and J.P. Wieleczko, *Phys. Lett. B* **390** (1997) 41
 22. R. Wada, R. Tezkratt, K. Hagel, F. Haddad, A. Kolomiets, Y. Lou, J. Li, M. Shimooka, S. Shlomo, D. Utley, B. Xiao, N. Mdeiwayeh, J.B. Natowitz, Z. Majka, J. Cibor, T. Kozik, and Z. Sosin, *Phys. Rev. C* **55** (1997) 227
 23. J. Bondorf, R. Donangelo, I.N. Mishustin, and H. Schulz, *Nucl. Phys. A* **444** (1985) 460
 24. D. Hahn and H. Stöcker, *Nucl. Phys. A* **476** (1988) 718
 25. J. Konopka, H. Graf, H. Stöcker, and W. Greiner, *Phys. Rev. C* **50** (1994) 2085
 26. T. Möhlenkamp, PhD thesis, Universität Dresden, 1996, unpublished
 27. J.P. Bondorf, A.S. Botvina, A.S. Iljinov, I.N. Mishustin, and K. Sneppen, *Phys. Rep.* **257** (1995) 133
 28. J. Hubele, P. Kreuzt, J.C. Adloff, M. Begemann-Blaich, P. Bouissou, G. Immé, I. Iori, G.J. Kunde, S. Leray, V. Lindenstruth, Z. Liu, U. Lynen, R.J. Meijer, U. Milkau, A. Moroni, W.F.J. Müller, C. Ngô, C.A. Ogilvie, J. Pochodzalla, G. Raciti, G. Rudolf, H. Sann, A. Schüttauf, W. Seidel, L. Stuttgé, W. Trautmann, and A. Tucholski, *Z. Phys. A* **340** (1991) 263
 29. J. Pochodzalla et al., *Proceedings of the 1st Catania Relativistic Ion Studies: Critical Phenomena and Collective Observables*, Acicastello, 1996, edited by S. Costa, S. Albergo, A. Insolia, and C. Tuvé (World Scientific, 1996) p. 1
 30. G. Immé et al., *Proceedings of the 1st Catania Relativistic Ion Studies: Critical Phenomena and Collective Observables*, Acicastello, 1996, edited by S. Costa, S. Albergo, A. Insolia, and C. Tuvé (World Scientific, 1996) p. 143
 31. C.A. Ogilvie, J.C. Adloff, M. Begemann-Blaich, P. Bouissou, J. Hubele, G. Immé, I. Iori, P. Kreuzt, G.J. Kunde, S. Leray, V. Lindenstruth, Z. Liu, U. Lynen, R.J. Meijer, U. Milkau, A. Moroni, W.F.J. Müller, C. Ngô, J. Pochodzalla, G. Raciti, G. Rudolf, H. Sann, A. Schüttauf, W. Seidel, L. Stuttgé, W. Trautmann, and A. Tucholski, *Nucl. Phys. A* **553** (1993) 271c
 32. G.J. Kunde, Diplomarbeit, Universität Heidelberg, 1990, report GSI-90-19
 33. U. Milkau, PhD thesis, Universität Frankfurt, 1993, report GSI-91-34
 34. R. Bougault, J.P. Wieleczko, M. D'Agostino, W.A. Friedman, F. Gulminelli, N. Leneindre, A. Chbihi, A. Le Fèvre, S. Salou, M. Assenard, G. Auger, C.O. Bacri, E. Bisquer, F. Bocage, B. Borderie, R. Brou, P. Buchet, J.L. Charvet, J. Colin, D. Cussol, R. Dayras, E. De Filippo, A. Demeyer, D. Doré, D. Durand, P. Eudes, J.D. Frankland, E. Galichet, E. Genouin-Duhamel, E. Gerlic, M. Germain, D. Gourio, D. Guinet, P. Lattes, J.L. Laville, J.F. Lecomte, T. Lefort, R. Legrain, O. Lopez, M. Louvel, L. Nalpas, A.D. N'guyen, J. Péter, E. Plagnol, A. Rahmani, T. Reposeur, M.F. Rivet, M. Squalli, J.C. Steckmeyer, M. Stern, B. Tamain, L. Tassan-Got, O. Tirel, E. Vient, and C. Volant, *Proceedings of the XXXV International Winter Meeting on Nuclear Physics*, Bormio, 1997, edited by I. Iori (Ricerca Scientifica ed Educazione Permanente, Milano, 1997), p. 251
 35. H. Xi, M.J. Huang, W.G. Lynch, S.J. Gaff, C.K. Gelbke, T. Glasmacher, G.J. Kunde, L. Martin, C.P. Montoya, S. Pratt, M.B. Tsang, W.A. Friedman, P.M. Milazzo, M. Azzano, G.V. Margagliotti, R. Rui, G. Van-nini, N. Colonna, L. Celano, G. Tagliente, M. D'Agostino, M. Bruno, M.L. Fiandri, F. Gramegna, A. Ferrero, I. Iori, A. Moroni, F. Petruzzelli, and P.F. Mastinu, preprint MSUCL-1073 (1997)

36. A. Kolomiets, E. Ramakrishnan, H. Johnston, F. Gimeno-Nogues, B. Hurst, D. O'Kelly, D.J. Rowland, S. Shlomo, T. White, J. Winger, and S.J. Yennello, *Phys. Rev. C* **54** (1996) R472
37. Hongfei Xi, W.G. Lynch, M.B. Tsang, and W.A. Friedman, *Phys. Rev. C* **54** (1996) R2163
38. Z. Majka, P. Staszal, J. Cibor, J.B. Natowitz, K. Hagel, J. Li, N. Mde- wayeh, R. Wada, and Y. Zhao, *Phys. Rev. C* **55** (1997) 2991
39. F. Gulminelli and D. Durand, *Nucl. Phys. A* **615** (1997) 117
40. P. Désesquelles, J.P. Bondorf, I.N. Mishustin, and A.S. Botvina, *Nucl. Phys. A* **604** (1996) 183
41. A.S. Botvina and I.N. Mishustin, *Phys. Lett. B* **294** (1992) 23
42. H.W. Barz, W. Bauer, J.P. Bondorf, A.S. Botvina, R. Donangelo, H. Schulz, and K. Snepken, *Nucl. Phys. A* **561** (1993) 466
43. P. Kreuz, J.C. Adloff, M. Begemann-Blaich, P. Bouissou, J. Hubele, G. Immé, I. Iori, G.J. Kunde, S. Leray, V. Lindenstruth, Z. Liu, U. Lynen, R.J. Meijer, U. Milkau, A. Moroni, W.F.J. Müller, C. Ngô, C.A. Ogilvie, J. Pochodzalla, G. Raciti, G. Rudolf, H. Sann, A. Schüttauf, W. Seidel, L. Stuttgé, W. Trautmann, and A. Tucholski, *Nucl. Phys. A* **556** (1993) 672
44. W.A. Friedman, *Phys. Rev. C* **42** (1990) 667
45. G. Papp and W. Nörenberg, *APH Heavy Ion Physics 1* (1995) 241; *Proceedings of the International Workshop XXII, Hirschegg, 1994*, edited by H. Feldmeier and W. Nörenberg (GSI, Darmstadt, 1994) p. 87
46. K.B. Morley, K. Kwiatkowski, D.S. Bracken, E. Renshaw Foxford, V.E. Viola, L.W. Woo, N.R. Yoder, R. Legrain, E.C. Pollacco, C. Volant, R.G. Korteling, H. Breuer, and J. Brzychczyk, *Phys. Rev. C* **54** (1996) 737